

# THE RELIQUARY BUST OF SAINT LAMBERT FROM THE LIÈGE CATHEDRAL, BELGIUM: GEMSTONES AND GLASS BEADS ANALYSIS BY PXRF AND RAMAN SPECTROSCOPY\*

Y. BRUNI and F. HATERT†

*Laboratory of Mineralogy, University of Liège B18, B-4000 Liège, Belgium*

P. GEORGE

*Liège Treasure of the Cathedral, Rue Bonne Fortune 6 B-4000 Liège, Belgium*

and D. STRIVAY

*European Centre of Archaeometry, University of Liège, Liège, Belgium*

*The reliquary bust of Saint Lambert, hosted in the Treasure of the Liège Cathedral, was produced in the early 15<sup>th</sup> century. This exceptional goldsmithery piece is covered with gold-coated silver, and decorated by approximately 400 stones, analysed by Raman and pXRF techniques to determine their mineralogical and chemical composition. The results confirm the identification of one hundred pearls, twenty-six rock crystals, ten amethysts, two diamonds, and numerous glass beads with a green, blue, colourless, turquoise, orange or red colour. The glass beads show a soda-lime composition, confirming that they are contemporary of the bust and imported from Venice, as reported by historical sources. Orange beads show a lead composition and the red stone a triplet with quartz, indicating that they were added to the bust later. The cutting of gems and beads shows also a significant evolution. The metal contains approximately 60% of Au and 40% of Ag. The origin of gemstones was difficult to establish, due to the absence of characteristic trace elements, but the chemical elements used for the manufacture and colouring of the beads were determined. This study confirms the trade of stones between Liège and Venice during medieval times.*

**KEYWORDS:** RELIQUARY BUST, SAINT LAMBERT, LIÈGE, GEMSTONES, GLASS BEADS, RAMAN SPECTROSCOPY, PXRF

## INTRODUCTION

Lambert of Maastricht (ca 636–705), better known as Saint Lambert, was born in a rich family of Maastricht, converted for a long time to Christianity. During his adolescence, he received an education based on history and holy texts, thus introducing him to customs of the royal court and to the monastic discipline. Around 670, Saint Lambert became successor of Bishop Theodard of Maastricht, but he had to go seven years in exile to the Stavelot abbey in Ardenne; he was then reinstated as Bishop of Tongres-Maastricht by the mayor of the palace Pepin II. On an undetermined year between 699 and 705, on September 17<sup>th</sup>, Saint Lambert was murdered in Liège, and his mortal remains were buried in Maastricht. Thirteen years later, his successor, Saint Hubert, decided to bring the relics back to Liège, since many miracles were observed on the place where Saint Lambert was martyred (Kupper 1993, Kupper and George 2006).

\*Received 5 April 2019; accepted 25 October 2019

†Corresponding author: email fhatert@uliege.be

© 2019 University of Oxford

The veneration of holy relics increased considerably during the Middle Ages to become “the way to rise to God”. The Saint Lambert relics, symbol of the Liège miracles, were kept in different shrines that have become famous cult and pilgrimage locations (George 2013). At the end of the 15<sup>th</sup> century, Guy de Brimeu, governor of Liège, had the idea to create a reliquary bust for the Saint Lambert skull. In 1508, Erard de La Marck, Prince-Bishop of Liège, asked to the goldsmith Hans Von Reutligen to realise this bust and he offered gold, 10 kg of silver, and approximately 400 pearls and stones from Venice. The bust, inaugurated on the April 28<sup>th</sup>, 1512, is a piece of goldsmith’s art of late Gothic style, constituted by a wooden structure covered with gold-coated silver, pearls and stones (the term “stones” is used, in this paper, to designate indifferently gems and glass beads). Saint Lambert has a chasuble and a rational on the body, a mitre on the head, as well as an episcopal crosier and an open book in the right and left hands, respectively. His face, originally in silver, was painted in 1743, and then repainted over in the 19<sup>th</sup> century. The total height of the bust is 159 centimetres, and the head still contains the relics of the Saint Lambert skull. The bust, hosted in the Treasure of the Saint Paul Cathedral in Liège (Belgium), is mounted on a complex pedestal on which six important moments of his life (two miracles - exile to Stavelot – martyrdom – burial – translation of the body – glorification) are represented (Colman and Sneyers 1974, Colman 1981, Kupper and George 2006).

The reliquary bust of Saint Lambert was conceived as an assemblage of goldsmith’s items mounted on a wooden structure in order to be easily disassembled. All pieces are classified into 11 groups and numbered according to their location. The bust has been restored several times (1595, 1743, 1816, 1849, 1972) since its creation in 1512. The last restoration, between October 1971 and September 1972, had for objectives to improve the state of conservation and the knowledge about the bust (Colman and Sneyers 1974). A previous study had already been done by Colman (1966) but some details were still unknown; this author also reported some back cracks, as well as several pieces to be quickly replaced. During the investigation of 1971, some discoveries were made in addition to urgent restorations and cleaning, like the two hallmarks at the back of the bust. The first represents the Eagle of Aix-La-Chapelle (Aachen), where the bust was manufactured, and the second shows the “I” and “R” letters, crossed for the name of the author Hans (also known as Iohann) von Reutlingen. Writings attesting dates of previous restorations and/or disassembles were also found on the book (1849) and the wooden base (1816, 1849, 1946) (Colman and Sneyers 1974).

The past decades have seen an increasing interest in the investigation of ancient goldsmith’s items by modern archaeometric techniques. Several examples of these studies occur in the literature, as the Raman and XRF investigations of the Prague sceptre (Petrová *et al.*, 2012), and of the Messina and Paolo Orsi jewellery collections (Barone *et al.*, 2015, 2016). The reliquary bust of Saint Lambert, certainly the most emblematic pieces of the Liège Cathedral’s Treasure, was never investigated by these modern archaeometric techniques. The goal of the present paper is consequently to characterize the gemstones and glass beads decorating the reliquary bust, by using handheld Raman and X-ray fluorescence spectrometric methods. The chemical data measured on the glass samples will help us to understand the nature of colouring agents and of raw materials, and to confirm the commercial links that existed between Liège and Venice at that time.

#### MATERIALS AND METHODS

The reliquary bust of Saint Lambert is a precious object of large size that cannot be moved or damaged. The best methods for these archaeometric analyses are therefore Raman and X-ray

fluorescence spectrometries because they are portable and non-destructive. Approximately 400 gems and glass beads, showing various colours, shapes, sizes and cuttings, decorated the reliquary bust. They are positioned both on the mitre, chest, back, hands and shoulders of the reliquary.

The portable Raman spectrometer is an Enwave Optronics EZRAMAN-I-DUAL from the European centre of Archaeometry of Liège (Belgium). This fibre optic-based instrument is equipped with two light sources, a green Nd: YAG laser (532 nm) and a red diode source (785 nm), as well as with a CDD detector. A removable rubber tip is attached to the end of the optical fibre to protect the beam from ambient light, and to always keep a relatively constant sample-laser distance for repeated measurements. The Raman spectrometer has an adjustable power controller for each laser with a maximum output power of 400 mW and 100 mW for 785 nm and 532 nm, respectively. The laser power used for this study is between 10 and 40 mW. The spectral region recorded was between 100 and 3200  $\text{cm}^{-1}$  for the 785 nm laser, and between 100 and 4000  $\text{cm}^{-1}$  for the 532 nm laser. Consequently, spectral resolutions are different, namely 7 or 8  $\text{cm}^{-1}$ , for the 785 and 532 nm lasers, respectively. Typical data analysis times were 60–120 s. Raman spectra were recorded in the software in \*.txt format and then exported in Excel. The spectra were cut at 1400  $\text{cm}^{-1}$  (spectral region between 100 and 1400  $\text{cm}^{-1}$ ) for a better presentation and they were not subjected to any postacquisition data manipulation. The comparative Raman spectra came mainly from the website RRUFF (2019) and Culka and Jehlička (2019) for minerals and from Colomban *et al.* (2006), Colomban (2008) and Tournié (2009) for glass beads.

The portable X-ray fluorescence spectrometer (pXRF) is a Thermo Fischer Niton XL3t with a 'GOLDD' detector, from the Mineralogy Laboratory, University of Liège (Belgium). The pXRF was placed against the gem or glass bead and X-rays were generated when the nosecone was in direct contact with the surface. The X-ray spot size was 3 mm in diameter. The X-ray tube has an Ag anode of 50 kV and 200  $\mu\text{A}$ . The lightest detectable element is Mg, but without an helium flow, this element cannot be detected with a good precision. The standardization mode selected is the "Cu/Zn Mining", which includes all elements of interest for the analysis of historical glasses (E.g., Ca, P, K, Mg, Fe, Sr, As). This analysis mode uses four separate filters to determine the concentrations in percentage of elements: a high filter (15 s counting time), a main filter (15 s), a low filter (15 s), and a light filter (30 s), leading to a total measurement time of 75 s per analysis. The software utilizes a Fundamental Parameters algorithm to determine concentrations of each element. The spectra and concentration values obtained from the XLT3 were downloaded to a computer for analysis. The concentration values were multiplied according to a standard element oxide conversion table to produce a percentage by weight of each oxide, and then the values were normalized to 100 wt.%.

## RESULTS

### *Description of gems and glass beads*

The reliquary bust is decorated by ca. 400 gems, pearls, and glass beads: 86 are localized on the back of the reliquary, 120 on the mitre, 60 on the chest, 38 on the shoulders, and 18 on the hands and the book (Fig. 1; the exact nomenclature and position of the stones is available online as supplementary material). Smaller stones (between 70 and 90) are also covering the ear of wheat located in the right hand of Saint Lambert (Fig. 2A), as well as flowers located on the back of the reliquary.



Figure 1 Photographs of the reliquary bust of Saint Lambert. (A) Front view. (B) Back view. (C) Shoulders. (D) Hands and book. [Colour figure can be viewed at [wileyonlinelibrary.com](http://wileyonlinelibrary.com)]

The stones show various colours (red, pink, orange, colourless, blue, turquoise, purple, green or dark green), shapes (round, square, rectangular) and sizes. Three different types of cuttings were observed: cabochon (Fig. 2B, F), with a low number of facets (Figs. 2C, D, E), and with numerous facets (Figs. 2G, H). Approximately 30 medallions were also noted, constituted by doublets with a lower part in which a religious or mythological figure is represented, covered with an upper colourless glass (Fig. 2I). Stones occur in gold settings, generally fixed with four hooks located at the corners of square or rectangular stones (Figs. 2C, D, E), and with at least eight hooks situated all around for the round stones (Figs. 2F, H). Between the setting and the bust, several silver petals occur, characterized by various degrees of curvature and complexity (Figs. 2B, D, E, H, I). The majority of flowers show six petals, but some of them contain seven petals.



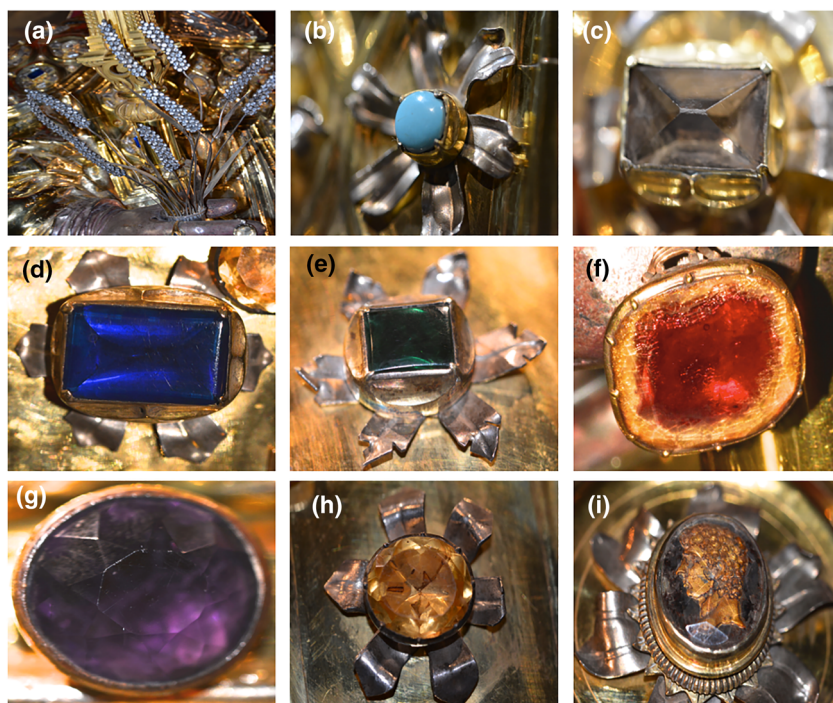


Figure 2 Detailed pictures of the stones occurring on the reliquary bust of Saint Lambert. (A) Ears of wheat, in the right hand of Saint Lambert. Several hundreds of colourless stones occur there. (B) Opacified turquoise glass bead, with a cabochon cutting, set with four hooks and decorated by six irregularly curved petals # D14. (C) Colourless quartz showing a simple 4-facets cutting and an hypothetic very narrow table (?). This rectangular stone is set by four hooks # D3. (D) Rectangular blue glass bead set by four hooks, and decorated by six simple petals. This cutting is characterized by a wide table, with curved edges # Pv7. (E) Rectangular green glass bead set by four hooks, and decorated by six complex petals. The cutting is similar to that of Figure 2D # D11. (F) Red stone, with a cabochon cutting, located on the right hand of Saint Lambert. The stone appear colourless on its borders # Blb5. (G) Amethyst showing a complex cutting with numerous facets. This stone is set without any hook # Mar1. (H) Orange glass bead with numerous facets, set with 8 hooks and decorated by six strongly curved petals # D9. (I) Glass medallion representing a mythological figure, set without any hook and decorated with six curved and complex petals # Epg centre. [Colour figure can be viewed at [wileyonlinelibrary.com](http://wileyonlinelibrary.com)]

### Raman spectroscopic analyses

Because of their too small size or their inaccessibility, it was impossible to analyse all stones. Moreover, the high values of fluorescence and absorption in dark coloured stones made the analyses sometimes difficult to obtain. These phenomena are common in handheld instrumentation (Jehlička *et al.* 2011). Some stones of each colour could thus be analysed, except for too small pink. A list of the Raman bands observed for all samples is available as supplementary material (Table 3).

The spectra of blue, green and dark green stones are relatively similar (Fig 3A), characterized by broad bands, confirming the amorphous nature of these phases. Blue glass beads show main bands located at  $534\text{ cm}^{-1}$  and  $1084\text{ cm}^{-1}$ , whereas green and dark green beads show main bands at  $536\text{ cm}^{-1}$  and at  $1080$  and  $1086\text{ cm}^{-1}$ , respectively (Fig. 3A). These spectra are in good agreement with all Raman signatures spectra of “ $\text{Na}_2\text{O} + \text{K}_2\text{O} + \text{CaO}$ ” glasses from Colomban *et al.* (2006). The bands between  $300$  and  $600\text{ cm}^{-1}$  correspond to the symmetric bending

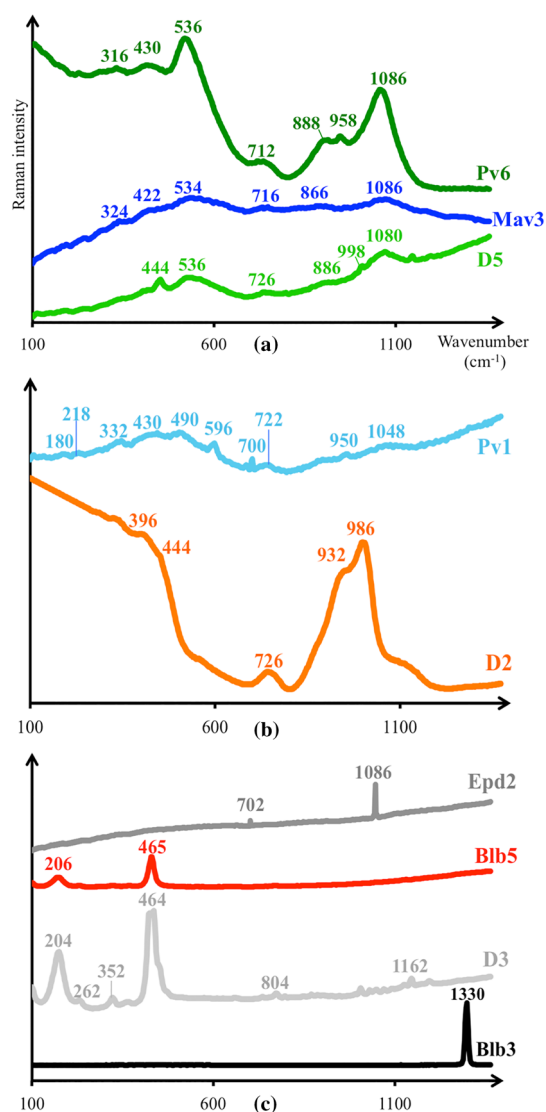


Figure 3 Raman spectra of the stones decorating the reliquary bust of Saint Lambert. (A) Dark green beads (# Pv6), blue beads (# Mav3) and green beads (# D5). (B) Turquoise beads (# Pv1) and orange beads (# D27). (C) Pearls (# Epd2), red quartz (# Blb5), colourless quartz (# D3) and diamond (# Blb3). [Colour figure can be viewed at [wileyonlinelibrary.com](http://wileyonlinelibrary.com)]

vibrations of the  $\text{SiO}_4^{4-}$  tetrahedra, while the bands between  $900$  and  $1300\text{ cm}^{-1}$  are assigned to the stretching vibrations of mainly depolymerised silicate (Robinet *et al.* 2008, Koleini *et al.* 2017). The band around  $1000\text{ cm}^{-1}$  is also certainly influenced by a fluorescence phenomenon because of the dark colour of the stones (Jehlička *et al.* 2011).

The spectra of orange glass beads show broad bands, confirming also the amorphous nature of these stones. The profile is however quite different from blue, green and dark green glass beads. The main band is located at  $986\text{ cm}^{-1}$ , accompanied by an intensity decrease of  $300\text{--}600\text{ cm}^{-1}$

regions (Fig. 3B). All orange Raman spectra are in very good agreement with the high lead silicate glasses spectra reported by Robinet *et al.* (2008) and Colomban *et al.* (2006).

The large majority of turquoise stones cannot be analysed with the Raman technique because of the very high fluorescence and the quick saturation. The spectrum of Figure 3B shows, however, ten weak and broad bands (180, 218, 332, 430, 490, 596, 700, 722, 950 and 1048  $\text{cm}^{-1}$ ). This spectrum is very different from those found in the RRUFF database for turquoise mineral, thus indicating that these samples are constituted by opacified glass beads or glazed ceramic.

Spectra of diamonds contain a single peak located at 1330  $\text{cm}^{-1}$  (Fig. 3C), in good agreement with the spectra published in the RRUFF database (RRUFF 2019) and by Culka and Jehlička (2019). Raman spectra of diamond are very characteristic, the signal is typically strong, and no laser-induced fluorescence was observed.

Six samples of quartz were analysed by Raman spectroscopy: four colourless (rock crystal), one purple (amethyst), and one red sample. Spectra obtained reveal a strong peak located between 462 and 465  $\text{cm}^{-1}$ , surrounded by other less intense peaks (Fig. 3C). These spectra are in good agreement with spectra from the RRUFF database (RRUFF 2019) and from Culka and Jehlička (2019), thus confirming the identification of these gemstones. All spectra for the different quartz samples are fluorescence-free.

Concerning pearls, Raman spectra show two characteristic bands; the strongest peak located at 1086  $\text{cm}^{-1}$ , and a less intense peak located at 702  $\text{cm}^{-1}$  (Fig. 3C). All pearls spectra are fluorescence-free.

#### *Chemical characterization by portable X-ray fluorescence spectrometry*

Chemical analyses of the stones and noble metals were performed with a pXRF spectrometer; the results are given in Tables 1 and 2. As for Raman spectrometry, it was impossible to analyse all stones due to the difficult access to certain part of the bust, or their too small size. Some analyses were also omitted because of their poor quality. Sodium was not directly measured, but according to the Raman spectra (see below), the glass beads are predominantly of soda-lime composition. Consequently, the  $\text{Na}_2\text{O}$  contents of Table 1 are constrained between 10 and 15 wt.%, in agreement with the literature for ancient soda-lime glasses (Nenna *et al.* 1997, Schalm *et al.* 2007, Tournié 2009, Verità 2013, Van Wersch *et al.* 2014, Silvestri *et al.* 2018). For turquoise beads, a  $\text{Na}_2\text{O}$  content between 10 and 15 wt.% was confirmed by Thornton *et al.* (2014), and for orange lead-bearing glass, sodium was considered as absent in agreement with previous analyses (Dungworth and Brain 2009) and the figure 5 (see discussions). Arsenic was not measured in Pb-bearing glass, due to XRF interference between these chemical elements.

The gemstones observed on the reliquary bust are diamond, rock crystal (colourless quartz), smoky quartz, amethyst and “pearl”. Diamond does not show any element in the analyses, since this mineral only contains carbon, which is not measured by pXRF (Table 1). Smoky quartz, rock crystal and amethysts show  $\text{SiO}_2$  contents very close to 100.00 wt.%, but minor amounts of  $\text{Al}_2\text{O}_3$  (< 0.63 wt.%) and  $\text{P}_2\text{O}_5$  (< 0.51 wt.%) were observed in some samples (Table 1). Pearls contain approximately 96 to 98 wt.%  $\text{CaO}$ , with significant amounts of  $\text{MnO}$  reaching 0.34 wt.% (Table 1).

The blue and green glass beads, as well as the medallions, show compositions characterized by ca. 5 to 10 wt.%  $\text{CaO}$ ,  $\text{Na}_2\text{O}$  between 10 and 15 wt.%,  $\text{K}_2\text{O}$  between 1.7 and 5 wt.%, and a very low  $\text{PbO}$  content (Table 1, Fig. 4A and 4B). According to the classification proposed by Tournié (2009), these glasses show a soda-lime composition. It is noteworthy that the compositions of dark green glass beads show significant differences, compared to the compositions of medallions,

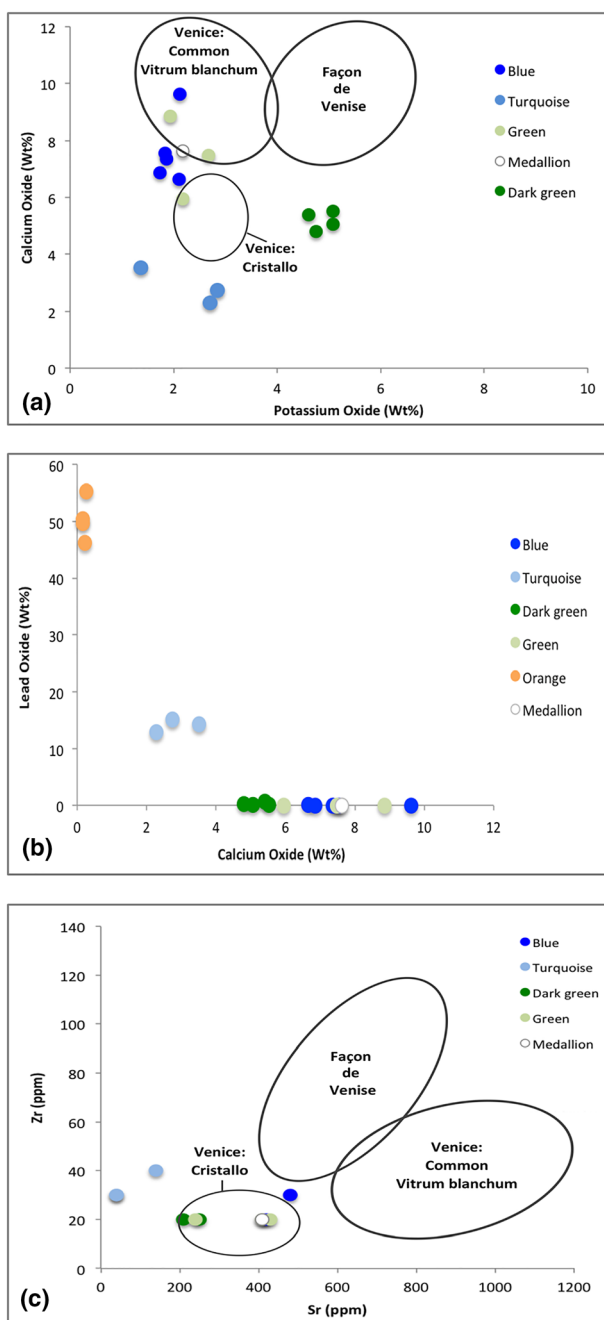


Figure 4 Correlations between some oxide contents in the glass beads from the reliquary of Saint Lambert, determined by pXRF. (A)  $MgO$  vs.  $CaO$ . (B)  $K_2O$  vs.  $CaO$ . (C)  $PbO$  vs.  $CaO$ . [Colour figure can be viewed at [wileyonlinelibrary.com](http://wileyonlinelibrary.com)]



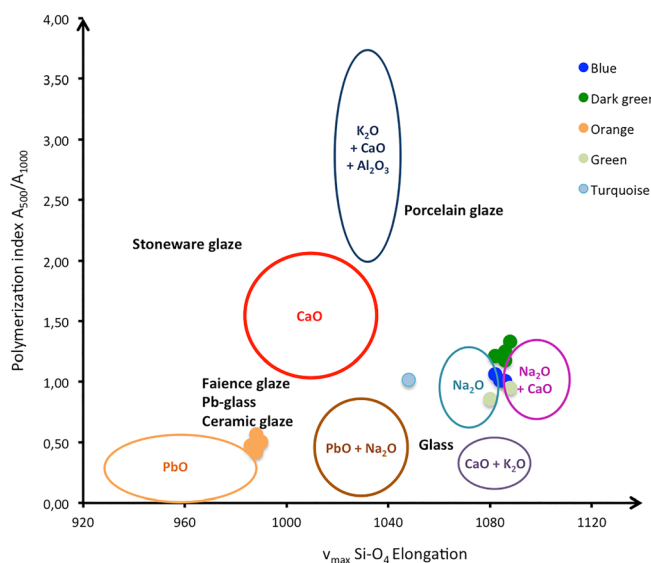


Figure 5 Classification of the different types of glasses, from their Raman spectral features (modified from Colomban *et al.*, 2006, and Colomban, 2008). Coloured dots correspond to the glass samples from the reliquary of Saint Lambert. [Colour figure can be viewed at [wileyonlinelibrary.com](http://wileyonlinelibrary.com)]

green beads, and blue beads. Indeed, they contain higher  $K_2O$  and  $Fe_2O_3$  around 4–6 wt.% and 2–3 wt.% respectively; lower  $CaO$  around 5 wt.%, as well as significant amounts of  $CuO$  reaching 1.34 wt.% (Table 1).

The orange glass beads show high amounts of  $PbO$  between 46 and 55 wt.% (Table 1 and Fig. 4B), thus indicating that they correspond to lead glass, according to Schalm *et al.* (2007). Compared to the compositions of other beads, they show higher  $MgO$  (3 to 4 wt.%) and  $K_2O$  (3 to 5 wt.%), and lower  $CaO$  (below 0.5 wt.%), (Table 1).

Turquoise glass beads show an intermediate  $PbO$  composition between the  $PbO$ -rich orange beads and the other glass beads; this is clearly shown in Figure 4B. They also contain lower  $CaO$  (2 to 4 wt.%) (Fig. 4A), and higher  $CuO$  (between 2 and 4 wt.%), and  $SnO_2$  (between 9 and 10 wt.%) (Table 1).

The red stone Blb5 shows an unusual composition, with 100.00 wt.%  $SiO_2$  (Table 1), thus indicating that it certainly corresponds to a quartz sample. This colour does not occur for natural quartz crystals, thus indicating that this sample was artificially coloured, as observed by Demaude (2016) and Demaude *et al.* (2017) on a medieval reliquary cross. Analyses of noble metals (Table 2) indicate that the gold samples contain 54 to 60 wt.%  $Au$ , 35 to 43 wt.%  $Ag$ , and 0.5 to 2.5 wt.%  $Cu$ . The silver samples, mainly constituting the petals, contain 79 to 85 wt.%  $Ag$ , 13 to 18 wt.%  $Au$ , and 2.8 to 3.2 wt.%  $Cu$ .

## DISCUSSIONS

### Correlation between Raman spectra and glass composition

Raman spectra of blue, green and dark green beads correspond to the Raman spectra signature of  $Na_2O$  or  $Na_2O/CaO$  glasses, while the orange glass spectrum is similar to that of  $Pb$ -glass

(Figs. 3A and B) (Colomban *et al.* 2006, Robinet *et al.* 2008, Tournié *et al.* 2010). Moreover, Colomban *et al.* (2006), Colomban (2008) and Tournié (2009) established several correlations between the chemical compositions of the flux and the Raman spectral data of ancient glasses. Starting from the polymerization degree of the glass (estimated from the amplitude ratio between the bands around 500 and 1000  $\text{cm}^{-1}$ ,  $A_{500}/A_{1000}$ ) and from the position of the stretching Si-O vibration band around 900–1100  $\text{cm}^{-1}$ , these authors published diagrams allowing to qualitatively estimate the chemical composition of a glass. Figure 5 shows the positions of our samples, reported on the flux diagram from the literature. It clearly appears that the green, dark green and blue glass beads show a composition close to the soda-lime field. This observation is in good agreement with the pXRF analyses, which show CaO contents between 4.81 and 8.85 wt.% for green and dark green glass beads, and between 6.65 and 9.63 wt.% for blue glass beads (Table 1). Orange beads are close to the PbO field, corresponding to the high PbO contents (46 to 55 wt.%) observed for these samples. The only turquoise bead analysed shows a glass composition between “PbO + Na<sub>2</sub>O” and “Na<sub>2</sub>O” fields, in good agreement with the pXRF analyses (Table 1) (Colomban *et al.* 2006, Tournié 2009, Colomban 2013).

### *Origin and dating of glass beads*

Due to their colours and lustre, gem materials are fascinating; for that reason, they were always used as medium of exchange or decoration. Very soon in history of humankind, gems were imitated by cheaper coloured glass, even in the Middle Ages when glass beads were frequently used to replace gems (Cannella 2006). Glass gem imitations are manufactured from three main components: the glass former agent, the flux, and the stabilizer. Sometimes an opacifier can also be added to produce an opaque glass (Cannella 2006, Verità 2014).

The glass former agent was only sand to the 14<sup>th</sup> century, but the Fe impurities of this material frequently produced strong undesired tints. For that reason, crushed pure quartz pebbles were also used in Venice from the 14<sup>th</sup> century (Cannella 2006, Rasmussen 2012, Moretti and Hreglich 2013).

Flux were constituted by natron (Na<sub>2</sub>CO<sub>3</sub>·10H<sub>2</sub>O) during the Roman and post-Roman periods (100 BC to 800 AD), then by plant and wood ashes from 800 AD to 1800 AD (Foy 2000, Picon and Vichy 2003, Moretti and Hreglich 2013). The natron and coastal plant ashes produced soda-lime glasses, while wood and continental plant ashes produced potash-lime glasses (Velde 2013, Verità 2013, Verità 2014). Stabilizers are necessary to decrease the solubility of the glass material in water and avoid devitrification; this stabilization is achieved by adding Mg, Ca, or Al to the glass (Cannella 2006, Navarro and Villegas 2013).

Opaque glasses were obtained by suspension of crystals in a glass matrix, such as tin oxide, and calcium or lead-antimonate (Ricciardi *et al.* 2009). Antimony-based opacifiers (lead antimonate for yellow and calcium antimonate for white) were used from around 1500 BC in the Near East and Egypt (Mass *et al.* 1998, Arletti *et al.* 2006, Ricciardi *et al.* 2009, Arletti *et al.* 2011). In about the 3<sup>rd</sup> century AD, it has gradually been replaced by tin dioxide (white opacifier) or lead stannates (yellow opacifier) from the eastern Mediterranean through into northern Europe. (Henderson 2000, Mirti 2002, Tite *et al.* 2008, Greiff 2008, Arletti *et al.* 2011).

The reliquary bust of Saint Lambert was manufactured between 1508 and 1512, and a very detailed drawing realized by Michel Natalis in 1653 clearly shows that the majority of glass beads (except orange beads) were already present on the bust at that time. The glass beads decorating the bust were consequently manufactured during the 16<sup>th</sup> or 17<sup>th</sup> centuries. The green, dark green, blue and turquoise glass beads, as well as the medallions, show compositions with Na<sub>2</sub>O = 10–

15 wt.%,  $K_2O = 1.5\text{--}5$  wt.%, and  $CaO = 2.5\text{--}10$  wt.% (Table 1), corresponding to soda-lime glass, with PbO between 13 and 15 wt.% for turquoise beads (Table 1). However, during that period, the glass produced in north-western Europe was of potash-lime composition, since the flux was constituted by wood and continental ashes (Velde 2013, Verità 2013). The only exception was glass beads from Venice, where the flux was Na-rich coastal plant ashes originating from Syria, Egypt or Spain (Cannella 2006, Velde 2013, Moretti and Hreglich 2013, Verità 2013). The Venetian soda glass was widely used from the 15<sup>th</sup> to the 17<sup>th</sup> centuries (Verità 2013; Verità 2014), but after that period, it was progressively replaced by K-rich Bohemian glass, *Façon de Venise* glass, and Pb-rich English glass (Smit *et al.* 2004, Cílová and Woitsch 2012, Verità 2013, Verità 2014).

The chemical compositions of the glass beads of the Saint Lambert reliquary are in very good agreement with those of the glass from Venice, indicating a possible origin for these samples (Fig. 4A) (Verità 2013, Verità 2014). This origin is confirmed by historical sources, since Colman and Sneyers (1974) and George (2013) indicate that the Prince-bishop Erard de La Marck bought pearls and “gemstones” for the manufacture of the reliquary in Venice in 1509. Variations of the absolute Raman intensities, between the spectra of dark green beads (high intensity; Fig. 3A) and those of green, blue and turquoise glass beads (low intensity; Figs. 3A and B), could be interpreted as different dates of production (Colomban 2008). However, this hypothesis is ruled out by the similar compositions of these glass beads, which confirm identical production periods.

The Zr and Sr content of glass beads is another argument, confirming their geographic origin. Indeed, the pXRF analyses clearly show Sr content between 200 and 500 ppm and Zr contents between 20 and 25 ppm for the glass beads, in good agreement with the range generally observed for authentic Venice glass, while glass “*Façon de Venise*” manufactured elsewhere in Europe (e.g., Antwerp, London) is significantly enriched in these two elements (De Raedt *et al.* 2002, Verità 2013) (Fig. 4C).

In turquoise beads, the presence of 9 to 10 wt.%  $SnO_2$  (Table 1) indicates that tin dioxide was used as opacifier, corresponding to a period between the 13<sup>th</sup> and the 19<sup>th</sup> centuries in Venice (Freestone and Bimson 1995, Thornton *et al.* 2014, Verità 2014).

In orange beads, the very high amounts of lead (45 to 55 wt. % PbO, Table 1) are similar to those of potassium-lead beads manufactured between the 17<sup>th</sup> and 18<sup>th</sup> centuries in Europe (Moretti 2003, Dungworth and Brain 2009, Kennedy *et al.* 2018). This relatively recent period of time is consistent with the absence of orange glass beads on the drawing of Michel Natalis (1653), as well as with the different cutting technique used for these glass beads (see below).

### *Relationship between chemical composition and glass colour*

The chemical data obtained by pXRF give us fundamental data to identify the materials that were used to give their colorations to the glass beads. Green glass beads show 0.22–0.27 wt.%  $Fe_2O_3$ , which are responsible for the colour (Cannella 2006, p. 186–187), while dark green glass beads show higher amounts of this element, between 2.18 and 2.52 wt.%  $Fe_2O_3$ , as well as significant contents in CuO (0.49–1.34 wt.%; Table 1). As mentioned by Verità (2013), Venetian dark green-coloured glasses generally contain Cu and Fe as colouring agents, and significantly high potassium contents (Table 1 and Fig. 4B).

Blue glass beads show significant copper and cobalt contents, in the ranges 0.06–0.17 wt.% CuO and 0.03–0.07 wt.% CoO (Table 1), indicating that either cobalt ore or more probably safre was used as colouring agent. This substance is a cobalt-rich glassy material imported from

Germany and added to obtain blue glass from the 14<sup>th</sup> to the 18<sup>th</sup> centuries (Cannella 2006, p. 162–163, Foy 2000). It is noteworthy that very small amounts of CoO, even below 0.05 wt.%, are sufficient to give a strong blue coloration to a glass (Biron *et al.* 1996, Cannella 2006, p. 163).

Turquoise glass beads show very high amounts of copper, lead and tin, in the ranges 2.76–4.04 wt.% CuO, 12.88–15.20 wt.% PbO, and 8.93–9.94 wt.% SnO<sub>2</sub> (Table 1). Copper oxide (generally 2 to >10 wt.% CuO) was commonly used to give the blue colour to turquoise glass in the Middle Ages (Biron *et al.* 1996, Cannella 2006, p. 160), and tin dioxide was added as opacifier agent (Henderson 2000, Mirti 2002, Tite *et al.* 2008, Greiff 2008, Arletti *et al.* 2011, Thornton *et al.* 2014, Verità 2014). The green tint induced by Fe<sub>2</sub>O<sub>3</sub> was certainly eliminated by adding MnO and As<sub>2</sub>O<sub>3</sub> (Steigenberger and Herm 2016).

Orange glass beads contain high amounts of lead (above 45 wt.%), potassium (3–5 wt.%), copper (0.03–0.08 wt.%), and manganese (0.20 wt.%). Copper nanoparticles (Cu<sup>0</sup>), associated to lead, are responsible for the colour (Cannella 2006 p. 146, Wedepohl 1995). Manganese was deliberately used as decolourizer, to remove the blue-green colour given naturally by iron oxide. The small amounts of manganese detected in orange glass beads show that the quantity of iron is very low (below the limit of detection) (Table 1) (Dungworth and Brain 2005).

The red stone, occurring on a ring of Saint Lambert, shows cracks and appears colourless on its borders, thus indicating that it is probably constituted by a triplet quartz/red glue/quartz (Fig. 2F). The absence of Raman characteristic bands of organic matter (Fig. 3C) and the 100% SiO<sub>2</sub> composition (Table 1) confirm that the red colouring agent is localized below the pure quartz table.

### *Evolution of cutting techniques*

The polishing of stones dates back to the 10<sup>th</sup> millennium BC, but technical improvements of the 4<sup>th</sup> century BC allowed to polish smaller objects, thus spreading the cabochon gem cutting all around the world (Bariand and Poirot 1998, Klein 2005). This cutting method gives nice colours to the gemstones and beads, and also allows keeping a maximal amount of material (Klein 2005, Cannella 2006). In Europe, simple faceting, with a large square or rectangular table surrounded by 4 facets, is known since the Middle Ages, but starting from the 14<sup>th</sup> century, more complex faceting techniques progressively appeared (Brose 1954, Klein 2005, Cannella 2006).

The stones observed on the reliquary bust of Saint Lambert were generally produced by very simple cutting techniques: turquoise, red quartz and medallions are always shaped in cabochons (Fig. 2B, F, I), and blue, green and dark green glass beads mainly show simple morphologies with a large table and four surrounding facets (Fig. 2D, E). Rock crystal samples, as well as some amethysts, also show similar simple shapes (Fig. 2C); a few glass beads are cut in cabochons. These simple faceting techniques correspond to those used when the reliquary was manufactured; this conclusion is confirmed by the drawing of Michel Natalis (1653), where these stones are clearly visible. A few stones, as for example the orange glass beads, are not reported on this drawing, and systematically show complex shapes with numerous facets (Fig. 2H). This complex cutting technique also observed on one amethyst sample (Fig. 2G) and on two rings, confirms the more recent origin of these stones.

Before the 9<sup>th</sup> century, diamonds were used in jewelry as transparent and unpolished crystals, but after this period in India, and from the 13<sup>th</sup> century in Europe, the technology of cleaving diamonds in octahedra and of removing deficiencies by polishing progressively appeared (Bariand and Poirot 1998, Klein 2005, Amar and Lev 2017). In the middle of the 15<sup>th</sup> century, Louis de Berquem, a Flemish jeweller, developed the scaif machine that allowed to obtain more precise



cuts, thus increasing the renown of diamonds (Cannella 2006, Amar and Lev 2017). The more complex brilliant cut appeared at the end of the 17<sup>th</sup> century (Klein 2005).

The two diamonds, observed on the rings decorating the right hand of Saint Lambert, show simple octahedral shapes (Fig. 1d), thus indicating that they are certainly contemporaneous with the bust. These rings are clearly visible on the drawing of Michel Natalis (1653).

### *Geographic origin of gemstones and pearls*

The gemstones decorating the reliquary are mainly constituted by rock crystal, smoky quartz, amethyst, diamond, and pearls. Historical sources describing the trade of gems during the Middle Ages are not abundant: best-quality gems were imported from Middle East, particularly from India (Brose 1954, Cannella 2006, Amar and Lev 2017), and they transited through Italy to reach European countries (Kunz and Stevenson 1908, Apellániz 2013).

Amethyst and rock crystal were very popular during the Middle Ages (Holmes 1934, Gontero-Lauze 2016, Amar and Lev 2017), because these cheap stones were mined in many European countries (e.g. France, Italy, Switzerland), as well as in Africa (e.g. Egypt) and in Asia (e.g. India, Iran, Syria) (Shaw 2000, Drauschke 2010, Van Roy 2011, Howard 2012). The origin of these gemstones is however very difficult to define, since quartz does not contain significant amounts of trace elements, as recently demonstrated by Delvaux (2018). All quartz were already present on the drawing of Michel Natalis (1653), except the red triplet and one amethyst (Fig. 2G–# MAR1) showing numerous complex facets and a simple setting.

Pearls were extremely popular during the Middle Ages; they represented ca. 75% of gem trade at that time. Pearls found in the Middle East (India, Sri Lanka, Persian Gulf) are rounded, with a shiny luster, slightly colored, and were collected in saltwater; pearls found in France and in Scotland are generally smaller, less transparent, less shiny, and were collected in rivers. Due to their poorer quality, European pearls were consequently cheaper and less prestigious; they were mainly used for ecclesiastic purposes. From the 17<sup>th</sup> century, the attractiveness of pearls decreased significantly, due to the development of faceted gemstones, as well as to the decrease of pearls natural abundance (Kunz and Stevenson 1908, Holmes 1934, Sirat 1968, Amar and Lev 2017). All pearls were already present on the drawing of Michel Natalis (1653).

The distinction between freshwater and saltwater pearls is possible thanks to their contents in Mn and Sr: Mn is higher in freshwater pearls, and Sr is higher in saltwater pearls (Habermann *et al.* 2001, Wehrmeister *et al.* 2007). According to the Mn/Sr diagram of Wehrmeister *et al.* (2007), pearls decorating the reliquary of Saint Lambert were of freshwater origin, due to their low strontium concentrations between 640 and 750 ppm, as well as to their high manganese concentrations between 400 and 1800 ppm. They certainly originate from Europe, and probably from Scotland since the pearls from Brittany (France) are of better quality and less abundant (Gontero-Lauze 2016).

The two diamonds occurring on the reliquary were already present on the drawing of Michel Natalis (1653), and their simple octahedral cut confirms their ancient origin. In the Middle Ages, diamonds were imported from India (Brose 1954, Klein 2005, Amar and Lev 2017), but also from Sri Lanka rivers (Amar and Lev 2017). It is impossible to determine the origin of the diamonds investigated here, due to the absence of characteristic trace elements in the pXRF analyses (Table 1).

## CONCLUSIONS

The reliquary bust of Saint Lambert is decorated by ca. 400 stones, mainly constituted by soda-lime glass beads with simple cutting. Their chemical composition indicates that they are contemporary to the reliquary, and that they were imported from Venice, as reported by historical sources. Orange stones with more complex facets do not appear on the drawing of Michel Natalis (1653), indicating that they were certainly added to the bust later. Their significant enrichment in Pb confirms that they were produced in more recent times.

The gemstones investigated herein are amethyst, rock crystal, diamond, pearls and a red colour quartz triplet; their geographic origin is very difficult to establish, due to the absence of characteristic trace elements. However, the archaeometric investigation of religious goldsmith artwork, with non-destructive techniques like pXRF or Raman spectrometry, is a necessary step to better understand the historical and geographic contexts in which these objects were produced.

## ACKNOWLEDGEMENTS

Merry Demaude and Nicolas Delmelle are acknowledged for their help during the Raman and pXRF analyses. We also thank the staff of the “Trésor de la Cathédrale de Liège” for their help in handling the reliquary bust of Saint Lambert.

## REFERENCES

- Amar, Z., and Lev, E., 2017, Most-cherished gemstones in the medieval Arab world, *Journal of the Royal Asiatic Society, Serie*, **3**(27/3), 377–401.
- Apellániz, F., 2013, Venetian trading networks in the medieval Mediterranean, *Journal of Interdisciplinary History*, **XLIV**(2), 157–79.
- Arletti, R., Ciarallo, A., Quartieri, S., Sabatino, G., and Vezzalini, G., 2006, Archaeometrical analyses of game counters from Pompeii, in *Geolaterials in cultural heritage* (eds. M. Maggetti and B. Messiga), 175–86, Vol. **257**, Special Publication of the Geological Society of London, London.
- Arletti, R., Vezzalini, G., Fiori, C., and Vandini, M., 2011, Mosaic glass from St Peter's, Rome: Manufacturing techniques and raw materials employed in late 16th-century Italian opaque glass, *Archaeometry*, **53**, 364–86.
- Bariand, P., and Poirot, J.-P., 1998, *Larousse des pierres précieuses*, 288, Larousse-Bordas, Paris.
- Barone, G., Bersani, D., Jehlicka, J., Lottici, P. P., Mazzoleni, P., Raneri, S., Vandenabeele, P., Di Giacomo, C., and Larinà, G., 2015, Nondestructive investigation on the 17-18th centuries Sicilian jewelry collection at the Messina regional museum using mobile Raman equipment, *Journal of Raman Spectroscopy*, **46**, 989–95.
- Barone, G., Mazzoleni, P., Raneri, S., Jehlicka, J., Vandenabeele, P., Lottici, P. P., Lamagna, G., Manenti, A. M., and Bersani, D., 2016, Raman investigation of precious jewelry collections preserved in Paolo Orsi regional museum (Siracusa, Sicily) using portable equipment, *Applied Spectroscopy*, **70**, 1420–31.
- Biron, I., Dandridge, P., and Wypyski, M.-T., 1996, Techniques and materials in Limoges enamels, in *Enamels of Limoges 1100–1350* (eds. B.-D. Boehm and E. Taburet-Delahaye), 48–62, The Metropolitan Museum of Art, New-York.
- Brose, H. W., 1954, A short history of faceting, *Lapidary Journal*, **2**, 446–52.
- Cannella, A.-M., 2006, *Gemmes, verre coloré, fausses pierres précieuses au Moyen Age*, Bibliothèque de la Faculté de Philosophie et, 480, University of Liège, Lettres.
- Cílová, Z., and Woitsch, J., 2012, Potash-a key raw material of glass batch for bohemian glasses from 14<sup>th</sup>-17<sup>th</sup> centuries? *Journal of Archaeological Science*, **39**, 371–80.
- Colman, P., 1966, *L'orfèvrerie religieuse liégeoise du XVe siècle à la Révolution*, Université de Liège, Liège.
- Colman, P., 1981, Le trésor de la Cathédrale Saint-Paul à Liège, *Feuilles archéologiques de la Société Royale Le Vieux Liège*, **14**, 1–9.
- Colman, P., and Sneyers, R., 1974, Le buste-reliquaire de Saint-Lambert de la Cathédrale de Liège et sa restauration, *Bulletin de l'institut royal du Patrimoine artistique*, **14**, 39–88.
- Colomban, P., 2008, On-site Raman identification and dating of ancient glasses: A review of procedures and tools, *Journal of Cultural Heritage*, **9**, e55–e60.

- Colomban, P., Tournié, A., and Bellot-Gurlet, L., 2006, Raman identification of glassy silicates used in ceramics, glass and jewellery: A tentative differentiation guide, *Journal of Raman Spectroscopy*, **37**, 841–52.
- Colomban, P., 2013, Non-destructive Raman analysis of ancient glasses and glazes, in *Modern Methods for Analysing Archaeological and Historical Glass* (ed. K. Janssens), 275–300, Vol. 1, Wiley, Chichester.
- Culka, A., and Jehlička, J., 2019, A database of Raman spectra of precious gemstones and minerals used as cut gems obtained using portable sequentially shifted excitation Raman spectrometer, *Journal of Raman Spectroscopy*, **50**, 262–80.
- De Raedt, I., Janssens, K., and Veeckman, J., 2002, On the distinction between 16th and 17th century venetian and *façon de Venise* glass, in *Majolica and glass, from Italy to Antwerp and Beyond: The Transfer of Technology in the 16<sup>th</sup>-early 17<sup>th</sup> Century* (ed. J. Veeckman), 95–121, Antwerpen City Press, Antwerp.
- Delvaux, C., 2018, L'intaille en améthyste de Hesbaye: étude minéralogique et gemmologique, 60, University of Liège, Master thesis.
- Demaude, M., 2016, Etude gemmologique de pièces d'orfèvrerie du Trésor de la Cathédrale Saint-Paul de Liège, 81, University of Liège, Master thesis.
- Demaude, M., Bruni, Y., Hatert, F., and Strivay, D., 2017, Etude gemmologique de la Croix-reliquaire à double traverse du Trésor de la Cathédrale de Liège, *Bulletin trimestriel du Trésor de Liège*, **50**, 9–15.
- Drauschke, J., 2010, Byzantine jewellery? Amethyst beads in east and west during the early byzantine period, *Intelligible Beauty*, **50–60**.
- Dungworth, D., and Brain, C., 2005, Investigation of late 17<sup>th</sup> century crystal glass, *Centre for Archaeology Report*, English Heritage, 21, 1–51.
- Dungworth, D., and Brain, C., 2009, Late 17<sup>th</sup> century crystal glass: An analytical investigation, *Journal of Glass Studies*, **51**, 111–37.
- Foy, D., 2000, Technologie, géographie, économie: Les ateliers verriers primaires et secondaires en occident. Esquisse d'une évolution de l'Antiquité au Moyen âge, in *La Route du verre. Ateliers primaires et secondaires du second millénaire avant J.-C. au Moyen Age* (ed. M.-D. Nenna), TMO 33, 147–70, Maison de l'Orient, Lyon.
- Freestone, I. C., and Bimson, M., 1995, Early venetian enamelling on glass: Technology and origins, in *Materials issues in art on archaeology* (eds. P. B. Vandiver, J. R. Druzik, J. L. Madrid, I. C. Freestone, and G. S. Wheeler), 415–31, Materials research society symposium proceedings, Vol. **352**, , Pittsburgh, PA.
- George, P., 2013, Le trésor des reliques de la Cathédrale de Liège, *Bulletin de l'institut archéologique liégeois*, **117**, 63–141.
- Gontero-Lauze, V., 2016, *Les pierres du Moyen Âge*, 222, Les Belles Lettres, Paris, France.
- Habermann, D., Banerjee, A., Meijer, J., and Stephan, A., 2001, Investigation of manganese in salt- and freshwater pearls, *Nuclear Instruments and Methods in Physics Reserach, B*, **181**, 739–43.
- Henderson, J., 2000, *The science and archaeology of materials: An investigation of inorganic materials*, 334, Routledge, London.
- Holmes, T., 1934, Mediaeval gem stones, *The University of Chicago Press on behalf of the Medieval Academy of America*, **9**(2), 195–204.
- Howard, M. C., 2012, *Transnationalism in ancient and medieval societies: The role of cross-border trade and travel*, 289, McFarland & Compagny, Jefferson, North Carolina, USA.
- Jehlička, J., Culka, A., Vandenabeele, P., and Edwards, H. G. M., 2011, Critical evaluation of a handheld Raman spectrometer with near infrared (785 nm) excitation for field identification of minerals, *Spectrochimica Acta Part A: Molecular and Biomolecular Spectroscopy*, **80**, 36–40.
- Kennedy, C. J., Addyman, T., Murdoch, K. R., and Young, M. E., 2018, 18<sup>th</sup> and 19<sup>th</sup> century Scottish laboratory glass: Assessment of chemical composition in relation to form and function, *Journal of Glass Studies*, **60**, 253–67.
- Klein, G., 2005, *Faceting history: Cutting diamonds & colored stones*, 242, Xlibris Corporation, USA.
- Koleini, F., Colomban, P., Antonites, A., and Pikirayi, I., 2017, Raman and XRF classification of Asian and European glass beads recovered at Mutamba, a southern African middle iron age site, *Journal of Archaeological Science*, **13**, 333–40.
- Kunz, G. F., and Stevenson, C. H., 1908, *The book of the pearl: The history, art, science, and industry of the queen of gems*, 552, The Century Company, New York, USA.
- Kupper, J.-L., 1993, Saint Lambert de l'histoire à la légende, *Feuillets de la Cathédrale de Liège*, **9**, 1–6.
- Kupper, J.-L., and George, P., 2006, *Saint-Lambert: de l'histoire à la légende*, 96, La Renaissance du Livre, Bruxelles.
- Mass, J. L., Stone, R. E., and Wypyski, M. T., 1998, The mineralogical and metallurgical origins of Roman opaque colored glasses, in *The prehistory and history of glassmaking technology, Ceramics and civilization* (eds. W. D. Kingery and P. McCray), 121–44, American Ceramics Society, Westerville, Ohio (USA).

- Moretti, C., 2003, English lead crystal: A critical analysis of the formulation attributed to George Ravenscroft – With points not yet clear on the process for the manufacture of “flint” glass, in *Annales du 16e congrès de l'Association Internationale pour l'Histoire du verre*, 223–6, 459, Nottingham.
- Moretti, C., and Hreglich, S., 2013, Raw materials, recipes and procedures used for glass making, in *Modern Methods for Analysing Archaeological and Historical Glass* (ed. K. Janssens), 30–7, Vol. 1, Wiley, Chichester.
- Nenna, M.-D., Vichy, M., and Picon, M., 1997, L'atelier de verrier de Lyon, du 1er siècle apr. J.-C., et l'origine des verres “romains”, *Revue d'archéométrie*, **21**, 81–7.
- Petrová, Z., Jehlicka, J., Capoun, T., Hanus, R., Trojek, T., and Goliás, V., 2012, Gemstones and noble metals adorning the sceptre of the Faculty of Science of Charles University in Prague: Integrated analysis by Raman and XRF handheld instruments, *Journal of Raman Spectroscopy*, **43**, 1275–80.
- Picon, M., and Vichy, M., 2003, D'Orient en Occident: l'originedu verre à l'époque romaine et Durant le haut Moyen Age, in *Echanges et Commerce du verre dans le monde antique* (eds. D. Foy and M.-D. Nenna), 17–31, actes du colloque international de l'AFAV en juin 2001, Aix-En-Provence et Marseille, Vol. **t.24**, Monographies Instrumentum, Montagnac.
- Rasmussen, S. C., 2012, *How glass changed the world: The history and chemistry of glass from antiquity to the 13<sup>th</sup> century*, 85, Springer, New-York.
- Robinet, L., Bouquillon, A., and Hartwig, J., 2008, Correlations between Raman parameters and elemental composition in lead and lead alkali silicate glasses, *Journal of Raman Spectroscopy*, **39**, 618–26.
- RRUFF, 2019, Integrated database of Raman spectra, <http://rruff.info/>
- Schalm, O., Janssens, K., Wouters, H., and Caluwé, D., 2007, Composition of 12–18<sup>th</sup> century window glass in Belgium: Non-figurative windows in secular buildings and stained-glass windows in religious buildings, *Spectrochimica Acta*, **B62**, 663–8.
- Silvestri, A., Gallo, F., Maltoni, S., Degryse, P., Ganio, M., Longinelli, A., and Molin, G., 2018, Things that travelled: A review of the Roman glass from northern Ardiatic Italy, in *Things that travelled* (eds. D. Rosenow, M. Phelps, A. Meek, and I. Freestone), 346–67, UCL Press, London.
- Sirat, C., 1968, Les pierres précieuses et leurs prix au XVe siècle en Italie, d'après un manuscrit hébreux, *Annales, Economies, Société, Civilisations*, **5**, 1067–85.
- Smit, Z., Janssens, K., Schalm, O., and Kos, M., 2004, Spread of façon-de-Venise glassmaking through central and western Europe, *Nuclear Instruments and Methods in Phys. Research B*, **213**, 717–22.
- Steigenberger, G., and Herm, C., 2016, Investigation of coloured lead glass glitter from an early eighteenth century material collection, Cambridge, by electron microscopy/energy dispersive X-ray analysis, *Heritage Science*, **4**(24), 1–9.
- Thornton, D., Freestone, I., Gudenrath, W., Bertini, M., Meek, A., and Ling, D., 2014, Thechnical study of a rare venetian turquoise glass goblet from the Waddesdon bequest, *The British Museum Technical Research Bulletin*, **8**, 1–1.
- Tite, M., Pradell, T., and Shortland, A., 2008, Discovery, production and use of tin-based opacifiers in glasses, enamels and glazes from the late iron age onwards: A reassessment, *Archaeometry*, **50**, 67–84.
- Tournié, A., 2009, Analyse Raman Sur site de verres et vitraux anciens: modélisation, procédure, lixiviation et caractérisation, PhD thesis, Université Pierre et Marie Curie, Paris, 162.
- Tournié, A., Prinsloo, L. C., and Colomban, P., 2010, *Raman spectra database of the glass beads excavated on mapungubwe hill and k2, two archaeological sites in South Africa*, University of Pretoria Internal Report, HAL.
- Van Roy, S., 2011, Considérations Sur les pierres précieuses du XIIIe siècle au travers des œuvres d'Hugo D'Oignies conservées à Namur, *Actes de la Journée d'étude Hugo D'Oignies contexte et perspectives*, TreMa, 205–23.
- Van Wersch, L., Biron, I., Neuray, B., Mathis, F., Chêne, G., Strivay, D., and Sapin, C., 2014, Les vitraux alto-médiévaux de Stavelot (Belgique), *ArchéoSciences*, **38**, 219–34.
- Velde, B., 2013, Glass compositions over several millennia in the Western world, in *Modern Methods for Analysing Archaeological and Historical Glass* (ed. K. Janssens), 64–78, Vol. 1, Wiley, Chichester.
- Verità, M., 2013, Venetian soda glass, in *Modern Methods for Analysing Archaeological and Historical Glass* (ed. K. Janssens), 515–36, Vol. 1, Wiley, Chichester.
- Verità, M., 2014, Secrets and innovations of Venetian glass between the 15<sup>th</sup> and 17<sup>th</sup> centuries: Raw materials, glass melting and artefacts, *Atti dell' Istituto Veneto di Scienze, lettere ed arti*, **172**, 53–68.
- Wehrmeister, U., Jacob, D. E., Soldati, A. L., Hager, T., and Hofmeister, W., 2007, Vaterite in freshwater cultured pearls from China and Japan, *Journal of Gemmology*, **31**, 269–76.



SUPPORTING INFORMATION

Additional supporting information may be found online in the Supporting Information section at the end of the article.

Table 3: List with all Raman bands of gemstones and glass beads. Numbers in bold denote strong bands.